TU/e EINDHOVEN UNIVERSITY OF TECHNOLOGY

Dynamic dilution effect in binary blends of linear polymers with well-separated molecular weights

Citation for published version (APA):
Ruymbeke, van, E., Shchetnikava, V., Matsumiya, Y., & Watanabe, H. (2014). Dynamic dilution effect in binary blends of linear polymers with well-separated molecular weights. *Macromolecules*, *47*(21), 7653-7665. https://doi.org/10.1021/ma501566w

DOI:
10.1021/ma501566w

Document status and date:
Published: 01/01/2014

Document Version:
Publisher's PDF, also known as Version of Record (includes final page, issue and volume numbers)

Please check the document version of this publication:

• A submitted manuscript is the version of the article upon submission and before peer-review. There can be important differences between the submitted version and the official published version of record. People interested in the research are advised to contact the author for the final version of the publication, or visit the DOI to the publisher's website.
• The final author version and the galley proof are versions of the publication after peer review.
• The final published version features the final layout of the paper including the volume, issue and page numbers.

Link to publication

General rights
Copyright and moral rights for the publications made accessible in the public portal are retained by the authors and/or other copyright owners and it is a condition of accessing publications that users recognise and abide by the legal requirements associated with these rights.

• Users may download and print one copy of any publication from the public portal for the purpose of private study or research.
• You may not further distribute the material or use it for any profit-making activity or commercial gain
• You may freely distribute the URL identifying the publication in the public portal.

If the publication is distributed under the terms of Article 25fa of the Dutch Copyright Act, indicated by the "Taverne" license above, please follow below link for the End User Agreement:

www.tue.nl/taverne

Take down policy
If you believe that this document breaches copyright please contact us at:

openaccess@tue.nl

providing details and we will investigate your claim.

Download date: 05. Oct. 2023

Macromolecules

Article

pubs.acs.org/Macromolecules

Dynamic Dilution Effect in Binary Blends of Linear Polymers with Well-Separated Molecular Weights

E. van Ruymbeke,*[,†] V. Shchetnikava,[‡,∥] Y. Matsumiya,[§] and H. Watanabe[§]

[†]Bio and Soft Matter, Institute on Condensed Matter and Nano-science, Université catholique de Louvain, Louvain-la-Neuve, Belgium

[‡]Department of Mathematics and Computer Science, Eindhoven University of Technology, Eindhoven, The Netherlands

[§]Institute for Chemical Research, Kyoto University, Gokasyo, Uji, Kyoto 611-0011, Japan

[∥]Dutch Polymer Institute (DPI), P.O. Box 902, 5600 AX Eindhoven, The Netherlands

ABSTRACT: We investigate and model the viscoelastic properties of binary blends composed of linear chains. These systems are indeed very suitable to test the validity and the limit of the constraint release (CR) process and dynamic tube dilution and to determine the value of the dynamic dilution exponent α. We first focus on binary blends containing *barely* entangled short chains. In such a case, we show that the tension re-equilibration process previously observed [van Ruymbeke et al. *Macromolecules* **2012**, *45*, 2085] can be correctly described as a *CR-activated* contour length fluctuation (CLF) process, which takes place along the fully dilated tube and is governed by the intrinsic Rouse time of a long−long entanglement segment. In addition, reptation is considered to take place along the fully dilated tube. We also show that this CR-activated CLF process speeds up the relaxation of the long chains, which naturally leads to an *effective* dilution exponent α equal to 4/3, despite the fact that the modeling is based on $\alpha = 1$. This result is in agreement with the experimental data. Then, we analyze the rheological behavior of binary blends containing entangled short chains. In such a case, we show that the CR-activated CLF also takes place, but with a *delay time* being necessary for the long chain to explore the dilated tube. This approach is tested for several binary blends, showing an improved quality of the predictions compared to previous tube modeling on the same blends. Indeed, by considering the chain motions on two different length scales, a larger fraction of the long chains relax at intermediate frequencies (through the tension re-equilibration) before their reptation, leading to an effective dilution exponent larger than 1 as determined from the low-frequency plateau modulus.

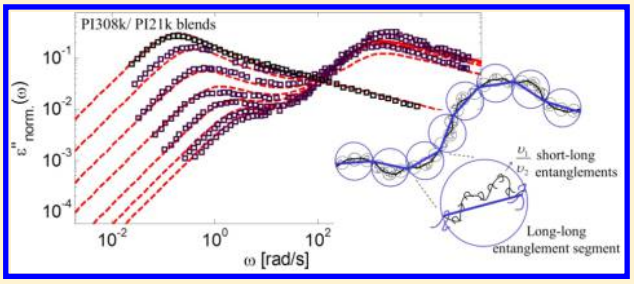

I. INTRODUCTION

These past years, a lot of progress has been made in order to understand and model the linear viscoelastic response of linear or branched polymer melts. In this direction, tube-based models serve as a powerful tool to predict the rheology of such systems from their composition.[1−4] Introduced by de Gennes and Doi and Edwards,[5−7] this coarse-grained model was initially based on two main relaxation mechanisms: the reptation of the chain along its primitive path and the contour length fluctuation (CLF).[7] Since then, this model has been more and more refined in order to also account for the influence of the molecular environment on the relaxation of a specific chain. Mechanisms such as the constraint release (CR), double reptation,[8,9] and/or dynamic tube dilution (DTD)[10−12] have been proposed, which allow reaching a quantitative level of prediction for a variety of polymers.

Despite this large success, however, fundamental questions remain to be addressed. In particular, the DTD/CR effect coming from fast motion of the short component on the relaxation has not been fully understood.[13−23] A major unsolved question is the exact value of the dynamic dilution exponent α, ranging between 1 and 4/3, is still not clear, despite its importance in the tube theory.[20,21,24] Indeed, within the tube picture, the normalized viscoelastic relaxation function of a polymer melt, $\mu(t)$, is defined as the product of the survival fraction of the dilated tube defined in the initial state (as an envelope of entanglement segments coarse-grained later at time t) $\varphi'(t)$ and the CR term, $\{\phi(t)\}^{\alpha}$, with $\phi(t)$ being an effective fraction of the initial constraints that survive at time t, as summarized in the expressions of $\mu(t)$ and the effective tube diameter $a(t)$:[1,3,25−28]

$$a(t) = a_0\{\phi(t)\}^{-\alpha/2} \tag{1}$$

$$\mu(t) = \varphi'(t)\{\phi(t)\}^{\alpha} \tag{2}$$

Here, a_0 indicates the initial, undiluted tube diameter (at $t = 0$), and $\{\phi(t)\}^{-\alpha}$ is the number of entanglement segments *per* dilated segment ($\{\phi(t)\}^{-\alpha}$ is equilavent to $\beta(t)$ in the previous work[16,17,29]). The value of this dilution exponent will therefore

Received: July 30, 2014
Revised: September 26, 2014
Published: October 21, 2014

ACS Publications © 2014 American Chemical Society

have a large consequence on the relaxation function of polydisperse polymers.

As shown for example in refs 14, 15, 25, 27, and 30−33, for most of the branched architectures, tube-based models have to use a value of $\alpha = 1$ in order to correctly fit the experimental data. However, several studies have shown that α is close to 4/3 for entangled polymers in solution.[24,34−36] Colby and Rubinstein also proposed $\alpha = 4/3$, based on the assumption that an entanglement is created from a fixed number of binary contacts between the chains.[34] They could therefore estimate the size of the "blob" needed in order to contain one effective entanglement *in a fully equilibrated state*, which was proportional to $1/{v_2}^{2/3}$, with v_2 being the volume fraction of the polymer. On the other hand, for hierarchically branched model polymers, several studies revealed that the low-frequency plateau of the storage modulus does not show unique dependence on the fraction of inner generations and scales as $\{\varphi'\}^{1+\alpha}$ with α varying from 1 to 4/3.[30] Therefore, the approach utilizing those model polymers did not allow extracting a unique value for α. Results obtained with multichain slip-link simulations[37] were also surprising: The simulation considered the entanglement as binary contacts of the chains (which corresponds to $\alpha = 1$), but the resulting low-frequency plateau of binary blends of linear chains scaled as $\{\varphi'\}^{7/3}$ (which gives the effective $\alpha = 4/3$).

Attempting to unify all these results, van Ruymbeke et al.[20,21] have recently proposed that the dynamic dilution exponent should be, for all systems, equal to 1: the fact that in specific cases this exponent seems to be larger than 1 is due to an additional relaxation process, which is not taken into account in the current tube models and which can lead to more significant relaxation of the slow component, compared to the relaxation predicted by the tube models.[20] Because of this extra relaxation process, the low-frequency plateau modulus is lower than expected, leading to an experimentally observed *effective* α larger than 1. This larger dilution effect was attributed to the tension re-equilibration process along the long chain, which was first proposed by Watanabe et al.:[38] for binary blends with widely separated component relaxation times, the blinking feature of release/re-formation of the short−long entanglements between the short and long chains leads to partial disorientation of the primitive path of the long chain within its dilated tube. Therefore, this process loosens some initial long−long entanglements only through the motion/relaxation of the short chains. (This feature is not taken into account in the present tube models giving eq 2.) As shown in refs 20 and 21, the tension re-equilibration time, τ_{TE}, is rather long, and in most of the cases, this mechanism is not effective, thereby giving the effective α equal to 1. However, in bidisperse blends of linear chains having *widely separated* molecular weights, that mechanism strongly influences the viscoelastic response of the long component, and therefore, different values of the *effective* dynamic dilution exponent can be observed, while keeping $\alpha = 1$ as the unique value describing the dilution of entanglements. In this paper, we further investigate this idea and see how the tension re-equilibration process could be modeled in a simple way to be incorporated in the tube model.

In addition to its influence on the level of the low-frequency plateau modulus, the tension re-equilibration also affects the terminal relaxation time of the long chains and the survival fraction of initial tube segments $\varphi'(t)$. Indeed, the blinking feature of the release/formation of short−long entanglements will lead to new breathing modes of the long chains along the dilated tube occurring at the rhythm of the short−long entanglements release/formation, which will speed up the long chain relaxation. This effect, which mainly affects the relaxation time of the long component in binary blends with widely separated molecular weight,[16,17,42] is usually taken into account in tube models by considering the "solvent effect" of the short chains on relaxation of the long chains, in particular on their terminal relaxation time.[10,13−15] According to the original DTD picture, the reptation time should therefore scale as $\{a(t)\}^{-2} \sim \{\varphi'(t)\}^{\alpha}$ (cf. eq 1). However, Struglinsky and Graessley suggested that this solvent effect emerges only when the long chains can "explore" their dilated tube in time, i.e., only if the constraint release Rouse (CRR) time of the long chains, $\tau_{CRR}(M_1,M_2)$, is shorter than their reptation time in the undilated (skinny) tube.[13] In the *simplest* case, this criterion is cast in a form

$$Gr = \frac{3\tau_e {Z_2}^3}{\tau_{CRR}(M_1, M_2)} = \frac{3\tau_e {Z_2}^3}{\tau_1(M_1){Z_2}^2} = \frac{3\tau_e {Z_2}^3}{(3\tau_e {Z_1}^3){Z_2}^2} = \frac{Z_2}{{Z_1}^3} > 1 \tag{3}$$

Here, Z_2 is the number of entanglement segments per long chain, τ_1 ($\propto {M_1}^3$) the reptation time of the short chain, and τ_e the Rouse time of an entanglement segment. This idea was tested by Park and Larson on several binary blends of linear chains.[14,15] They concluded that, indeed, the short chains could not be considered as the solvent immediately after their relaxation. They also concluded that the DTD picture must be applied to the reptation of the long component as soon as its corresponding Graessley number, *Gr*, was larger than 0.064, rather than the initially proposed value of 1. Most of current tube models are based on a similar assumption: short chains fully act as a solvent for the reptation of the long chains if the long chains had enough time to explore their dilated tube. For bidisperse linear blends with widely separated component molecular weights, this criterion allows speeding up the long chain relaxation, thereby improving the agreement between the model predictions and experimental viscoelastic data.

However, several discrepancies still remain. These discrepancies were often attributed to the fact that the above approach considers only two "extreme" cases of reptation in a skinny tube or in a fully dilated tube.[14,15] One could indeed easily expect that in most of the cases reptation should happen along a partially dilated tube of diameter a^* with $a_0 < a^*(t) <$ fully dilated diameter $a(t)$. This goes along with the idea of Matsumiya et al., who recently showed that the relaxation of monodisperse linear polymers occur along the partially dilated tube that wriggles in the fully dilated tube of the diameter $a(t)$, while on the other hand, $\mu(t)$ and $\varphi'(t)$ of those polymers obey the full-DTD relationship $\mu(t) = \{\varphi'(t)\}^{1+\alpha}$ ($\varphi'(t) = \phi(t)$ in eq 2).[39] This result suggests that, on one hand, the stress level is essentially determined by the (local) equilibration of the chains in the direction perpendicular to their backbone multiplied by the tube survival fraction, while on the other hand, the long chain relaxation in the (partially) dilated tube requires first the chain tension along the whole tube axis to be re-equilibrated through the CR mechanism.

In this paper, we adopt a similar approach considering two different length scales (tube diameters) to describe two different quantities, the magnitude of the stress decay due to DTD on one hand and, on the other hand, the terminal relaxation time of the long component, which are related to the fully and partially dilated tube diameters, $a(t)$ and $a^*(t)$,

dx.doi.org/10.1021/ma501566w | Macromolecules 2014, 47, 7653−7665

respectively. In a real solvent, $a(t)$ and $a^*(t)$ coincide with each other.

Related to these two length scales, the molecular picture of partially dilated tube was recently extended to binary blends by Watanabe et al.,[21] who have examined the relaxation times of the components, considering that the mutually entangled long chains in the blend exhibit reptation/CLF along the partially dilated tube only after the CR-activated tension re-equilibration is completed. In the case of binary blends having well-separated component molecular weights, they have shown that the relaxation of the long component can indeed be well described by a *solution model*, which treats the blend as an equivalent solution but with the retardation due to this tension re-equilibration. In their work, the retardation factor was determined from the relaxation time data of the monodisperse components and the CR time data of the dilute long chain in the short chain matrix. This semiempirical approach allowed them to evaluate the main relaxation times of the components, but not the relaxation mode distribution (i.e., the relaxation time spectrum). In the present work, we would like to further investigate this idea but remove this limitation, thereby incorporating the idea in tube model calculation.

Thus, our first objective is to study how the tension re-equilibration process affects, in a self-consistent way, the CR mechanisms (see eq 2) and/or the relaxation times of the long chains. Contrary to the semiempirical approach in ref 21, we would like to look at the full relaxation time spectrum of the chains, not only its terminal time. To this end, we use the tube model with the time marching algorithm (TMA) to calculate the whole relaxation function (equivalent to the full spectrum) and separate the contributions from the reptation, contour length fluctuations (CLF), and CR mechanisms to the rheological response of the blends. This allows us to discuss the influence of the CR-activated tension re-equilibration process on each of these relaxation mechanisms as well as the cumulative effect of reptation and CLF processes on the terminal relaxation time of the long component. As mentioned in ref 21, the influence of the tension re-equilibration process can be considered by taking into account a fully/partially coarse-grained time scale and focusing on the terminal relaxation of the components occurring in the fully/partially dilated tube. In this study, we would like to describe the evolution of the surviving tube fraction in all time scales, from the short chain relaxation time up to the terminal time of the long chain, and discuss the results with respect to the theoretical works proposed by Doi et al.[40] and by Viovy et al.[41] for describing the constraint release mechanisms in the case of binary blends of linear chains. While according to Doi et al. the relaxed short chains are acting as a real solvent and the motions of the long chains are always considered along their fully dilated tube, Viovy et al. consider both the motions of the chain within the initial tube and the motions of this initial tube within the dilated tube, which take place at the rhythm of the short chains motions.

Our second objective is to incorporate the CR-activated tension re-equilibration process in the tube model. To this end, we propose to describe this process as an *extra*, CR-activated CLF along the dilated tube, which takes place in addition to "intrinsic CLF" along the skinny tube. This goes along with the observation of Wang et al.,[42] who suggested, based on experimental data of a large series of bidisperse linear samples, that the CLF process takes place depending on the proportion and length of the short chains. This idea was also proposed in refs 18 and 43. In particular, Read et al. proposed a new model, which accounts for "enhanced CLF" in the case of bidisperse systems. However, the complexity of their approach as well as the use of two adjustable parameters (that includes the dilution exponent α) does not allow us to easily see the consequence of these enhanced CLF. Following the idea proposed in ref 20, we fix the value of this exponent to $\alpha = 1$ and examine if the extra CR-activated CLF process along the (fully and/or partially) dilated tube leads to an enhanced effect of the relaxed short chains on the relaxation of the long chains and to the loss of some long−long entanglements before the reptation of the long chains.

For investigation of the CR/DTD effect(s) on the relaxation of the long chains, important information can be drawn from comparison of experimental viscoelastic ($\mu(t)$ in eq 2) and dielectric (close to $\varphi'(t)$ in eq 2) relaxation functions of the blends, as shown by Watanabe et al. for a series of model systems.[16,17,29,44−46] Therefore, in this study we confront the results obtained with our tube model to experimental viscoelastic data as well as these dielectric data. Differing from the previous study in which the viscoelastic moduli were calculated from the dielectric *data*, this study starts from a full model incorporating CR-activated CLF to calculate both viscoelastic moduli and dielectric loss simultaneously.

The paper is organized as followed. At first, in section II, the samples focused in this work are summarized. Then, in section III, we briefly present the tube model (formulated with the time marching algorithm (TMA)) used in this study.[27,47] Section IV presents/discusses the results of comparison of the model and data. We first focus on the viscoelastic response of bidisperse blends that contain barely entangled short chains and then examine the blends in which the short chains are entangled with the long chains. Conclusions are drawn in section V.

II. MATERIALS

Table 1 summarizes the linear polybutadiene (PBD) and *cis*-polyisoprene (PI) samples utilized in this study. The sample code number indicates the molar mass (M_w) in kg/mol. All of them were synthesized/characterized in previous studies. The blends of those samples were made at various volume fractions υ_2 of the long component. The rheological data (and also the dielectric data for PI blends) have been reported in the references given in Table 1.

Table 1. Characteristics of the Linear Samples

code	$10^{-3}M_w$	T (°C)	ref
PBD3	3.8	40	42
PBD410	411.5	40	42
PBD20	20.0	25	14
PBD550	550.0	25	14
PBD25	25.0	28	48
PBD160	160.0	28	48
PBD36	36.8	25	13
PBD168	168.0	25	13
PI21	21.4	40	16
PI308	308.0	40	16
PI14	14.0	40	49
PI329	329.0	40	49

III. MODELING

In order to model the relaxation in binary blends of linear chains, we use the time marching algorithm (TMA) developed

dx.doi.org/10.1021/ma501566w | Macromolecules 2014, 47, 7653−7665

in refs 27, 47, and 50. It must be noted however that the conclusion obtained with this model in the case of the bidisperse blends is not specific to the approach followed here and also holds for other tube models such as the hierarchical model proposed by the group of Larson and/or the model developed by the group of McLeish and Read. The main difference between TMA and the other tube models is probably the fact that CLF in TMA does not speed up the reptation time directly via shortening of the distance to reptate. In TMA, the CLF process influences the final relaxation time through eq 7 (see below).

III.1. Basic Modeling of Relaxation Modulus $G(t)$. The relaxation modulus $G(t)$ of the entangled polymer at time t includes both the fast Rouse relaxation function $G_R(t)$ and the slow entanglement relaxation function $G_d(t)$, the latter describing the reptation, CLF, and CR processes:[1,2,43,51]

$$G(t) = G_R(t) + G_d(t) \tag{4}$$

with

$$G_R(t) = \sum_k \frac{\upsilon_k \rho RT}{M_k}\left\{\frac{1}{4}\sum_{p=1}^{Z_k}\exp\left(-\frac{p^2 t}{\tau_R(M_k)}\right) + \sum_{p=Z_k+1}^{n}\exp\left(-\frac{2p^2 t}{\tau_R(M_k)}\right)\right\} \tag{5}$$

and

$$G_d(t) = G_N^0 \mu(t) = G_N^0 \varphi'(t)\{\phi(t)\}^{\alpha} \tag{6}$$

In eq 5, ρ, R, and T denote the polymer density, gas constant, and absolute temperature, respectively. The indices $k = 1$ and 2 stand for the short and long chains, respectively, and υ_k, M_k, and $\tau_R(M_k)$ represent the volume fraction, molecular weight, and longest Rouse relaxation time of the component k. In eq 6, G_N^0 denotes the plateau modulus, $\mu(t)$ is the normalized viscoelastic function of the blend as a whole (see eq 2), and $\{\phi(t)\}^{-\alpha}$ is the number of entanglement segments *per* dilated segment ($\{\phi(t)\}^{-\alpha}$ is equilavent to $\beta(t)$ in the previous work[16,17]). $\mu(t)$ is due to the contribution from the long and short components and given as an average for these components, as explained below for eq 7. The storage and loss moduli are obtained as the Fourier transformation of $G(t)$.

The survival fraction of the initial tube appearing in eq 6, $\varphi'(t)$, is determined by summing up, for all tube segments, the probability that the initial segment orientation still survives at time t, even after the reptation and CLF process of the chain:[27,52]

$$\varphi'(t) = \sum_k \upsilon_k \int_0^1 p_{rept}^{[k]}(x_i, t) p_{fluc}^{[k]}(x_i, t)\, dx_i \tag{7}$$

Here, $p_{rept}^{[k]}(x_i, t)$ and $p_{fluc}^{[k]}(x_i, t)$ respectively indicate the survival probabilities of the initial tube segments at the normalized position x_i at time t defined for the reptation and CLF processes of the chain component k. Similarly to the coordinate system used for describing the relaxation of star polymers,[11,12] x_i runs from 0 at the chain extremity to 1 at the chain center (from a modeling point of view, linear chains can be seen as two-arm star chains, able to reptate). Equation 7 is later modified to incorporate the CR-activated CLF (cf. eq 13).

As explained in detail in ref 52, the survival probabilities $p_{rept}^{[k]}(x_i,t)$ and $p_{fluc}^{[k]}(x_i,t)$ decay with respective characteristic reptation time $\tau_{rept}(M)$ and the early fluctuation time defined as a function of x, $\tau_{early}(x_i)$, as[53]

$$p_{rept}^{[k]}(x_i, t) = \sum_{q=\text{odd}} \frac{4}{q\pi}\sin\left(\frac{q\pi x_i}{2}\right)\exp\left(-\frac{q^2 t}{\tau_{rept}(M_k)}\right) \tag{8a}$$

with

$$\tau_{rept}(M) = 3\tau_e Z^3 \{\Phi^*\}^{\alpha} \tag{8b}$$

and

$$p_{fluc}^{[k]}(x_i, t) = \exp\left(\frac{-t}{\tau_{early}(x_i)}\right) \tag{9a}$$

with

$$\tau_{early}(x_i) = \frac{1}{2}\frac{9\pi^3}{16}\tau_e (Z/2)^4 x_i^4 \tag{9b}$$

τ_e is the Rouse relaxation time of the entanglement segment that serves as the minimum unit time for the entanglement relaxation.

The early fluctuation time $\tau_{early}(x_i)$ (eq 9b) is much shorter than the reptation time $\tau_{rept}(M_k)$ (eq 8b) for $x_i \cong 0$. Thus, the linear chains are assumed, in eqs 8 and 9, to relax at their extremities by the early, shallow intrinsic-Rouse fluctuation and at the remaining part, by reptation (with the intrinsic curvilinear diffusion coefficient), without the CR-activated CLF process. In eq 9b, a prefactor 1/2 has been considered in order to well describe the dielectric data, as discussed in section IV.1. The parameter Φ^* appearing in eq 8b determines the length $Za_0(\Phi^*)^{\alpha/2}$ of the (partially) dilated tube along which the chain reptates, while considering that the short chains are acting as a solvent. If the long chain reptates/fluctuates along the fully dilated tube, Φ^* is identical to the effective fraction of the initial constraints that survive at time t, $\phi(t)$ (= $\varphi'(t)$ for this case), as mentioned in the Introduction. However, in most of the cases, long chain needs some time before effectively moving along the dilated tube. Therefore, in the conventional tube model, Φ^* for the long chain in the bidisperse blend is often assumed to be equal to υ_2 if the components therein have widely separated molecular weights (based on the Struglinsky–Graessley criterion[13]); otherwise, the model assumes $\Phi^* = 1$. As discussed in section IV.3, the approach developed here is different and considers that the reptation of the long chains in a (either fully or partly) diluted tube can always take place, but at the rhythm of the release/reformation time of the short–long entanglements.

The effective fraction of the initial constraints that survive at time t, $\phi(t)$, being related to the tube diameter determining the stress level (see eq 1), is—in most of the cases—equal to the survival fraction of initial tube segments $\varphi'(t)$.[1,2] However, if a large fraction of the polymer suddenly relaxes, $\phi(t)$ should be larger, depending on the local CR equilibration time of a long–long entanglement segment, and specified as[25,28]

$$\phi(t) = \max\left\{\varphi'(t), \phi(t'')\left[\frac{t''}{t}\right]^{1/2}\right\} \tag{10}$$

Here, t'' represents a time just before t. The $[t''/t]^{1/2}$ factor appearing in eq 10 represents a decrease of ϕ for a case that the decay in the interval Δt from t'' (= $t - \Delta t$) to t occurs only

dx.doi.org/10.1021/ma501566w | Macromolecules 2014, 47, 7653–7665

through the constraint release Rouse (CRR) mechanism, as fully explained in Appendix of ref 20.

As in section III.2, some of the bidisperse blends that we would like to study contain barely entangling short matrix chains. Such short chains are regarded to relax through the intrinsic Rouse mechanism, and their contribution to the relaxation modulus $G(t)$ is specified as (instead of eq 5)[1]

$$G_k(t) = \frac{\upsilon_k \rho RT}{M_k} \sum_{p=1}^{n} \exp\left(-\frac{p^2 t}{\tau_R(M_k)}\right) \tag{11}$$

III.2. Incorporation of CR-Activated CLF of the Long Chains Blended with Barely Entangling Short Matrix Chains. As mentioned in the Introduction, we would like to incorporate in our tube model, in addition to the reptation and intrinsic Rouse-CLF of the long chains, the effect of the CR-activated tension re-equilibration process on the survival fraction of initial tube segments. As illustrated in Figure 1, the skinny tube itself is able to move in the dilated tube, due to the blinking feature of the release/re-formation of short−long entanglements.[20]

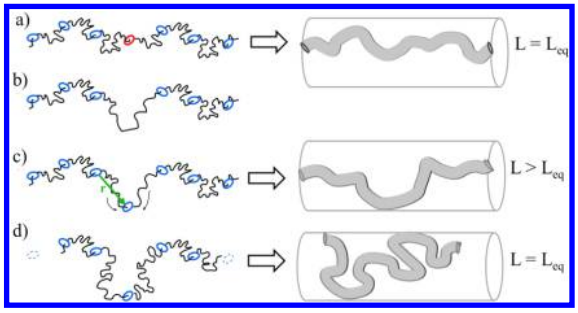

Figure 1. Illustration of the tension re-equilibration process along a long chain and corresponding tube pictures: (a) A long chain constrained by the other long chains and short chains. (b) The long chain starts exploring its dilated tube on local CR due to the short chain motion. (c) A long−short entanglement is transiently re-formed isotropically, which leads to tension imbalance along the long chain thereby activating the tension re-equilibration through the monomer transfer (sucking-in of monomers for the illustration here). At this stage, the equilibrium length of the primitive path of the long chain is longer than the initial equilibrium length. (d) For end-free long chain, the tension re-equilibration results in some loss of initial long−long entanglements.

Since the tension re-equilibration process is a Rouse process constrained by the long−long entanglements, we propose to describe it in a way similar to that for the early fluctuation (see eq 9). However, this process is now happening in a tube dilated by the short chains: the skinny tube (and the long chains therein) is fluctuating at the rhythm of the release/re-formation of the short−long entanglements. We therefore refer to this process as *CR-activated fluctuation* (CR-CLF).

In the extreme case of barely entangled short matrix chains having the longest relaxation time $\tau_1 \sim \tau_e$, the CR-CLF process of the long chains can be described by eq 9a with τ_{early} therein being replaced by

$$\tau_{CR\text{-}CLF}(x) = \frac{1}{2}(\tau_e \upsilon_2^{-2})\frac{9\pi^3}{16}(\upsilon_2 Z/2)^4 x^4 \tag{12}$$

Here, the factor $\tau_e \upsilon_2^{-2}$ represents the intrinsic Rouse equilibration time within long−long entanglement segment. This Rouse time comes from the fact that the molecular weight between two long−long entanglements, i.e., of the fully dilated tube segment, is equal to $M_{e0}\upsilon_2^{-1}$. Correspondingly, the number of long−long entanglement segments is equal to $\upsilon_2 Z$, which leads to the $(\upsilon_2 Z/2)^4$ scaling in eq 12: This $(\upsilon_2 Z/2)^4$ factor is smaller than the $(Z/2)^4$ factor appearing in eq 9b because the equilibrium length of the primitive path wriggling in the dilated tube is shorter than the initial primitive path defined along the skinny tube.

Thus, in this extreme case of barely entangling short matrix chains, eq 12 is equivalent to an expression of early fluctuations along the primitive path of the dilated tube, which leads to enhanced (CR-activated) fluctuations of the long chains and thus to an increased fraction of long chains relaxed before their terminal time (see section IV.2). On the contrary, for binary blends composed of well-entangled long and short linear chains, one expects that eq 12 is not valid anymore because the equilibration time within a long−long entanglement segment (determined by the motion of the short chains) becomes too large to be neglected. This point is further discussed in section IV.3.

In order to include the CR-activated CLF process in our tube model, the survival fraction of initial tube segments (see eq 7) is now described as

$$\varphi'(t) = \sum_k \upsilon_k \int_0^1 p_{rept}^{[k]}(x_i, t) p_{fluc}^{[k]}(x_i, t) p_{CR-CLF}^{[k]}(x_i, t)\, dx_i \tag{13}$$

Here, $p_{CR-CLF}^{[k]}(x_i,t)$ is the survival probability of the initial tube segments at the position x_i at time t defined for the CR-CLF process of the chain component k. For the short chain, the CR-activated CLF process is negligible, and thus we set $p_{CR-CLF}^{[1]}(x_i,t) = 1$. In contrast, for the long chain, this process should be important, and the probability for this chain is modeled in terms of the CR-CLF time (eq 12) as

$$p_{CR\text{-}CLF}^{[2]}(x_i, t) = \exp\{-t/\tau_{CR\text{-}CLF}(x_i)\} \tag{14}$$

Because of the $p_{CR\text{-}CLF}^{[2]}(x_i,t)$ term, $\varphi'(t)$ (eq 13) decays more significantly compared to that in the earlier model (eq 7): the chain extremities can indeed relax either by reptation, by the intrinsic-Rouse CLF, or by CR-CLF. We therefore expect a larger proportion of long chains to relax before their terminal relaxation, which should decrease the low-frequency plateau of the storage modulus of the blends. This point will be tested on experimental data in section IV.

Furthermore, thanks to the CR-activated CLF process, the long chains start exploring their dilated tube. Even if this process is not very rapid in the blends, one could expect that it shortens the terminal relaxation time of the long chain compared to the time in the monodisperse case. Also, for this category of bidisperse blends characterized by barely entangled short chains and a large Gr number, one can assume that the chains have time to move in their fully dilated tube before reptation occurs. Therefore, their reptation time is considered as proposed in eq 8b, with $\Phi^* = \upsilon_2$. Indeed, following a similar way as the one proposed in eq 12, the reptation time composed of Z_2 initial entanglement segments is determined as[10]

$$\tau_{rept}(M) = 3\left(\frac{\tau_e}{\upsilon_2^2}\right)(\upsilon_2 Z_2)^3 = (3\tau_e Z_2^3)\upsilon_2 \tag{15}$$

Material Parameters. The tube model formulated above contains three material parameters: the molecular weight

dx.doi.org/10.1021/ma501566w | Macromolecules 2014, 47, 7653−7665

between two entanglements M_{e0}, the Rouse time of an entanglement segment τ_e, and the plateau modulus G_N^0. These parameters have been fixed, for all blend samples, as indicated in Table 2, and in agreement with the values used in previous studies.[20,27,43,47]

Table 2. Material Parameters Utilized in the Model

	M_{e0} (g/mol)	τ_e (s)	G_N^0 (MPa)
polybutadiene blends	1650	3.0×10^{-7} (25 °C)	1.2
polybutadiene blends	1650	2.5×10^{-7} (28 °C)	1.2
polyisoprene blends	3800	4.5×10^{-6} (40 °C)	0.45

IV. RESULTS AND DISCUSSION

As described in the Introduction, the main objective of this study is to investigate and model the influence of the short chain motion on the relaxation time of the long chain as well as on the height of the low-frequency plateau of the storage modulus, i.e., on the effective value of the dilution exponent. To do so, both experimental viscoelastic and dielectric data are used. In the followings, we first validate our model by comparing predicted and experimental dielectric and viscoelastic data of monodisperse linear chains. Then, in section IV.2, we study the viscoelastic response of linear bidisperse blends in which the components have widely separated molecular weights and the short component is barely entangled, while in section IV.3, we investigate the rheology of bidisperse blends in which the short chains are also well entangled. All calculations are made for the fixed value of the dilution exponent, $\alpha = 1$.

IV.1. Dielectric and Viscoelastic Behavior of Monodisperse Linear Samples. As a first test, we analyze the viscoelastic and dielectric data of entangled linear polymers. As described in detail in refs 16, 17, and 39, the high-frequency Rouse dynamics (eq 5) and the DTD dynamics resulting from accumulation of local CR process, with the latter being represented by the $\{\phi(t)\}^\alpha$ factor for the viscoelastic $\mu(t)$ in eq 2, hardy affect the dielectric relaxation. Therefore, in order to calculate the dielectric relaxation function $\varepsilon(t)$, we can utilize the same equations as those for predicting the viscoelastic behavior, expect eq 2 that must be replaced by

$$\varepsilon(t) = \varepsilon_d(t) = \Delta\varepsilon\varphi'(t) \tag{16}$$

with $\Delta\varepsilon$ being the dielectric relaxation intensity. In eq 16, we have neglected a minor DTD contribution to $\varepsilon_d(t)$ (due to the chain motion within the edges of surviving portion of the dilated tube) and equate the normalized dielectric relaxation function, $\varepsilon_d(t)/\Delta\varepsilon$, to the survival fraction of the dilated tube, $\varphi'(t)$. The normalized dielectric loss, $\varepsilon_{norm}''(\omega) = \varepsilon''(\omega)/\Delta\varepsilon$, is given as the Fourier transformation of $\varepsilon_d(t)/\Delta\varepsilon$.

Based on these equations and on the material parameters given in Table 2 for polyisoprene samples, the predicted dielectric loss and viscoelastic moduli of five different linear samples (with M_w equal to 21, 43, 99, 179, and 308 kg/mol) are obtained and compared to experimental data in Figures 2 and 3. The agreement is very good, which validates—in the case of monodisperse linear chain—the full DTD picture with the dynamic dilution exponent α equal to 1, being in harmony with the conclusion found in ref 39. It must be noted that the slight discrepancy observed for the lowest molecular weight sample (M_w = 21 kg/mol, Z = 5.5 entanglements) is most probably due to the fact that our tube model considers that CLF process takes place already at time $t = 0$, i.e., before the time the chains need in order to reach their equilibrium state. In the case of poorly entangled chains, this speeds up the relaxation of the outer molecular segments, as it has been discussed in details in refs 50 and 52. Also, it is interesting to observe, on the dielectric data, the transition between the CLF modes (characterized by the characteristic slope proportional to $\omega^{-1/4}$) and the reptation peak: while nearly absent for the lower MW samples (which considerably relax by CLF), this transition is well pronounced for the high MW samples, in both the predicted and experimental data. Indeed, in this last case, only a small fraction of the chains is relaxing by CLF and the dominant relaxation process is the reptation.

As mentioned in section III.1, a prefactor 1/2 has been added in eq 9b in order to correctly describe the dielectric loss data. Indeed, as illustrated in Figure 2, without this prefactor, a small discrepancy is systematically observed either in the location of the reptation peak or in the fluctuations slope, independently from the value of the dilution exponent (1 or 4/3). While the origin of this factor 1/2 is not clear and needs to be further investigated, it could be related to the fact that early

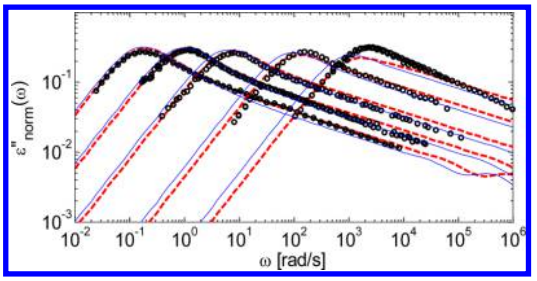

Figure 2. Comparison between calculated (curves) and measured (symbols) normalized dielectric loss for different monodisperse polyisoprene samples of average molecular weights (in weight) equal to 21, 43, 99, 179, and 308 kg/mol (from right side to left side). The calculation was made with $\Phi^* = 1$ in eq 8b and without considering CR-activated CLF. The early fluctuations times has been determined, following eq 9b, with (thick - - -) or without (thin - - -) considering a prefactor 1/2.

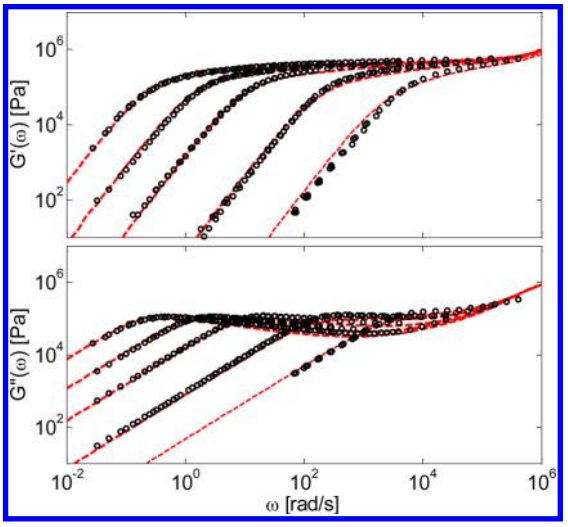

Figure 3. Comparison between calculated (curves) and measured (symbols) storage and loss moduli for different monodisperse polyisoprene samples of average molecular weights (in weight) equal to 21, 43, 99, 179, and 308 kg/mol (from right side to left side). The calculation was made with $\Phi^* = 1$ in eq 8b and without considering CR-activated CLF.

dx.doi.org/10.1021/ma501566w | Macromolecules 2014, 47, 7653−7665

fluctuations times have been determined, based on the rotational Rouse relaxation time $\tau_R^{(rot)}$, rather than on the shorter stress relaxation time ($= \tau_R^{(rot)}/2$).[53] It must be noted that this prefactor is not due to the coordinate system used for describing the linear chains (as two-arm star polymers), as it was observed in ref 54.

IV.2. Linear Bidisperse Blends with Well-Separated Molecular Weights, Containing Barely Entangled Short Chains. In this specific case, the long and short chains have very widely separated molecular weights, and the latter is barely entangled to behave essentially as a real solvent. For such blends, one might expect that tube model based on the full dynamic tube dilution (full-DTD) picture should adequately describe the experimental data (thus, using eqs 12, 13, and 15). We first test this idea for bidisperse blends of PBD3 and PB410,[42] the former having $M_1/M_{e0} = 2.3$.

The barely entangling short component, PBD3 (having $M \cong 2M_{e0}$), is assumed here to relax according to the Rouse dynamics (see eq 11). On the other hand, for the long chain, different options to determine the relaxation time are tested and discussed.

First, if we assume that the long chain relaxes by reptation along the skinny tube ($\Phi^*(t) = 1$ in eq 8b) and that the CR-activated CLF process is not involved (i.e., eq 7 is valid), the predicted relaxation of the long chains in the blend is too slow, especially for the blends containing a small fraction of long chains ($\upsilon_2 < 20\%$), as demonstrated in Figure 4.

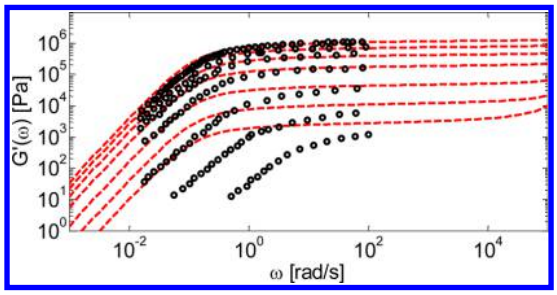

Figure 4. Comparison between calculated (curves) and measured (symbols) moduli for blends of PBD3 and PBD410 having various compositions, υ_2 (%) = 100 (bulk PBD410), 80, 60, 40, 20, 10, and 5. The calculation was made with $\Phi^* = 1$ in eq 8b and without considering CR-activated CLF.

The discrepancy which is seen at small υ_2 was already observed in the literature,[14,15] showing the importance of incorporation of the *dilution effect* of the short chains on the reptation time of the long chain (for the cases satisfying the Struglinsky–Graessley criterion, eq 3). Therefore, we followed usual model treatment to rescale the initial reptation time by the factor of $\Phi^*(t) = \upsilon_2$ (cf. eq 8b or eq 15).[14,15,48] Results of this calculation, still utilizing eq 7, are shown in Figure 5: The discrepancy becomes much smaller but still remains, as noted for the terminal regime and in particular, for the low-frequency plateau (too narrow mode distribution and too high plateau level for the calculation). This discrepancy is not specific to the tube model examined here but also found for the other versions of the model; see, for example, refs 14 or 15. It must be noted that an increase of the dynamic dilution exponent α only transposes the problem: For larger α, the low frequency data become better described by the model but a larger discrepancy emerges at intermediate frequencies.[48]

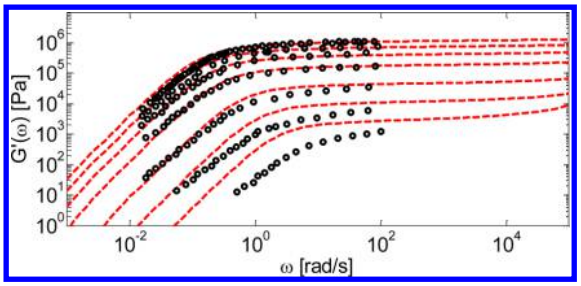

Figure 5. Comparison between calculated (curves) and measured (symbols) moduli for blends of PBD3 and PBD410 having various compositions, υ_2 (%) = 100 (bulk PBD410), 80, 60, 40, 20, 10, and 5. The calculation was made with $\Phi^* = \upsilon_2$ in eq 8b and without considering CR-activated CLF.

The above result is in harmony with the previous argument in ref 47 that the classical relaxation processes are not enough for describing the blend data and an extra relaxation process, allowing a smooth transition of the *effective* α (i.e., the value of α which would have been found from the level of the second plateau modulus), from 1 to 4/3 is necessary. As explained in the Introduction, this extra process is attributed to the CR-induced tension re-equilibration along the long chains due to fast release/re-formation of the long–short entanglements.[20,21,38] This extra process, leading to loss of long–long entanglements near the chain extremities, is described, in this study, as the CR-activated CLF process.

Since the barely entangled short chain (PBD3) can be regarded as a real solvent, we approximate the CR-activated CLF process as the intrinsic Rouse process having the long–long entanglement equilibration time as short as $\tau_e\upsilon_2^{-2}$; this point is further discussed later in section IV.3.4. For this case, eqs 12 and 13 can be used. The early relaxation of the long chain can then occur through two different fluctuation mechanisms, either the intrinsic CLF along the skinny tube or the CR-activated CLF along the dilated tube. Based on the Struglinski–Graessley criterion (eq 3), the long chains are assumed to reptate along the dilated tube (sustained only by the long chains), and we set $\Phi^* = \upsilon_2$ in eq 8b, while the modulus is calculated by combining eq 13 with eqs 6 and 10. The results, shown in Figure 6, very well agree with the data for all υ_2 values, lending support to the mechanism of CR-activated CLF. Specifically, it should be emphasized that the CR-activated CLF process accelerates the relaxation at the long chain extremities to reproduce the smooth decrease of the storage modulus to the low-frequency plateau with the height

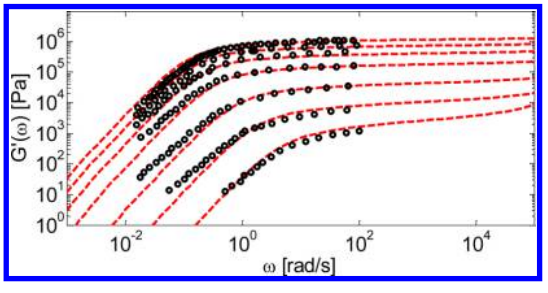

Figure 6. Comparison between calculated (curves) and measured (symbols) moduli for blends of PBD3 and PBD410 having various compositions, υ_2 (%) = 100 (bulk PBD410), 80, 60, 40, 20, 10, and 5. The calculation was made with $\Phi^* = \upsilon_2$ in eq 8b by considering the CR-activated CLF (eqs 12 and 13).

dx.doi.org/10.1021/ma501566w | Macromolecules 2014, 47, 7653–7665

being scaled as $\upsilon_2^{7/3}$. Namely, this process gives the effective dilution exponent >1 being consistent with experiments, despite the theoretical $\alpha = 1$ was utilized in the calculation.

The above results seem to support the idea that in the blends of barely entangled short chains and much longer chains the early relaxation of the long chain mainly occurs through the CR-activated CLF (tension re-equilibration) process along the fully dilated tube. This process significantly speeds up the relaxation at the long chain extremities, in agreement with experimental data.

IV.3. Linear Bidisperse Blends with Well-Separated Component Molecular Weights, Containing Well-Entangled Short Chains. Figure 6 has demonstrated that for binary blends with barely entangled short chains the time necessary for the relaxation within the long−long entanglement is close to $\tau_e\upsilon_2^{-2}$, and the tension re-equilibration process is well described by eq 12. However, this is not the case for blends containing well entangled short chains. Indeed, in such blends, the long chain should move along the dilated tube at the rhythm of the release/creation of the short−long entanglements, and this characteristic time should depend on the lifetime and concentration of these short−long entanglements, thereby retarding the relaxation within the long−long entanglement.[20,21]

In order to investigate this retardation, we first focus on the relaxation of the binary blends of PI21 and PI308 (with $M_1 \cong 5.5M_{e0}$; see Table 1).[16] The advantage of these blends is that both viscoelastic and dielectric data have been measured and analyzed. This allows us to compare measured and predicted data for both viscoelastic moduli and dielectric loss and thus to significantly minimize the possible sources of error since, as mentioned in section IV.1, dielectric data are insensitive to the high-frequency Rouse process and the DTD process.

IV.3.1. Test of Molecular Picture of Reptation along Fully Dilated Tube for PI/PI Blends. If we consider the reptation of the long component in a fully dilated tube as if the long chains were diluted in a real solvent (i.e., $\Phi^*(t) = \upsilon_2$ in eq 8b), we should obtain a too fast reptation process since the short chains considered here are entangled. This is indeed demonstrated in Figure 7, which compares literature data of dielectric loss of

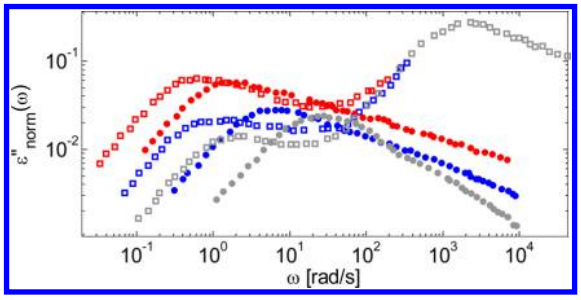

Figure 7. Comparison between normalized dielectric loss data for blends of PI21 and PI308 (open square) and PI308 diluted in real solvent (filled ○), at various compositions, υ_2 (%) = 20, 10, and 5.

these blends to the loss of the long component in a real solvent (oligomeric butadiene),[16] both reduced at an isofrictional state: The terminal time of the long chain is much shorter in the real solvent than in the PI21 matrix.

Keeping this in mind, we compare, in Figure 8, the experimental and calculated storage modulus and dielectric loss of these blends, the model calculation being performed with the assumption that the long chains reptate along the fully

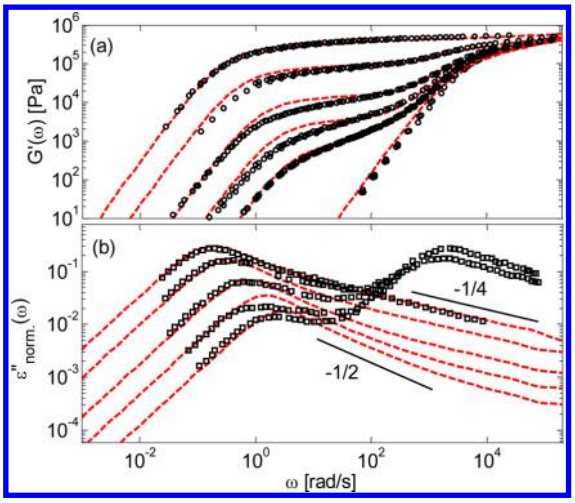

Figure 8. Comparison between experimental data (storage modulus (a) or normalized dielectric loss data (b)) and calculation for blends of PI21 and PI308 having various compositions, υ_2 (%) = 100, 50, 20, 10, and 5. The calculation was made with $\Phi^*(t) = \upsilon_2$ in eq 8b and without considering CR-activated CLF. For (b), the calculated curves only show the responses of the long chains.

dilated tube (i.e., $\Phi^*(t) = \upsilon_2$ in eq 8b) *without* being affected by the CR-activated CLF. (This assumption is similar to that in the calculation by Park and Larson and by several other groups for the viscoelastic modulus.[14,15]) In Figure 8b, the theoretical dielectric response only shows the contribution from the long chains (not of the blend as a whole). One can see that the agreement is not too bad, contrarily to our expectations from the comparison made in Figure 7. This is due to the fact that the too fast reptation of the long chains assumed in the calculation is, in this specific case, compensated by the too slow (quenched) CLF-CR process in the calculation, which leads to a too pronounced second plateau observed in the storage modulus. Because of this underestimation of the reptation time and overestimation of the CLF-CR process, one can see in Figure 8b that the power law behavior $\varepsilon_{norm}''(\omega) \propto \omega^{-1/4}$ characteristic of the early fluctuation process is experimentally observed at intermediate frequencies but not reproduced in the predicted curves in the right range of frequency, especially at low concentrations of long chains. In fact, this power-law behavior is calculated to emerge at much higher frequencies, $\omega \geq 10^4$ rad/s. As a consequence, the long chains are nearly not relaxing at intermediate frequencies, leading to this too pronounced second plateau. Thus, the calculation with the assumption of the long chains reptation along the fully dilated tube ($\Phi^*(t) = \upsilon_2$) not associated by the CR-activated CLF cannot reproduce the data at intermediate frequencies, no matter what the reptation time considered for the long chain is.

IV.3-2. Test of Molecular Picture of CR-Activated CLF for PI/PI Blends. The above results, together with the conclusion of section IV.2, suggest the importance of the CR-activated CLF of the long chains in description of the blend data. The relaxation of the short chains is indeed fast compared to the motion of the long chains, and motion of these short chains should lead to the tension re-equilibration along the long chains in some time scale. As a first trial, one may assume that the tension re-equilibration process is associated with the characteristic, intrinsic Rouse time given by eq 12 and that the long chain entangled with the short chains reptates along the fully dilated tube as considered in eq 15 (or, equivalently, with

dx.doi.org/10.1021/ma501566w | Macromolecules 2014, 47, 7653−7665

$\Phi^*(t) = \upsilon_2$ in eq 8b). The calculation based on these two assumptions is shown in Figure 9: The calculation excellently

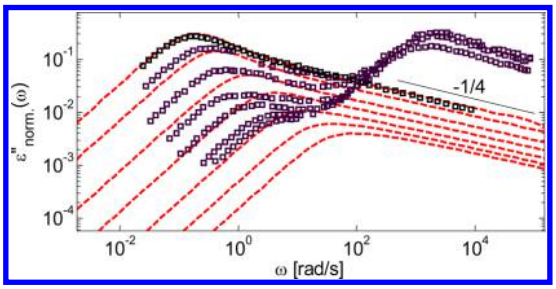

Figure 9. Comparison between calculation and data of normalized dielectric loss for PI21 and PI308 (see Table 1) mixed in different proportions: 100%, 50%, 20%, 10%, 5%, 3%, and 2% of PI308. The calculation was made with $\Phi^* = \upsilon_2$ in eq 8b and by considering the CR-activated CLF (eqs 12 and 13). The calculated curves show only the contribution of the long chains.

reproduces the shape of the ε'' curves. In particular, considering the CR-activated CLF mechanism suppresses the transition zone in which a power law behavior $\varepsilon_{norm}''(\omega) \propto \omega^{-1/2}$ was observed. However, the relaxation time of the calculated curve is clearly shorter than the data, and this difference becomes larger with decreasing concentration of the long chains in the blend.

From the results seen in Figure 9, one can conclude that long chains entangled with much shorter chains largely relax through CR-activated CLF, as expected, but this relaxation process takes place with a certain delay time that depends on the long chain concentration.[21] This delay naturally emerges because the short but well-entangled chains cannot behave as a solvent in the short time scale of $t = \tau_e$ (the time scale introduced for barely entangled short chains; cf. section IV.2). Consequently, eq 12 needs to incorporate a time $\tau_{long-long\ eql}$ necessary for one long–long entanglement segment to be internally relaxed/equilibrated and achieve the tension re-equilibration along the chain backbone. This time is equivalent to the onset time of CR-activated CLF. Since the long–long entanglement segment contains υ_1/υ_2 short–long entanglements each having an average lifetime $\tau_{short-long}$, and since the relaxation/equilibration within the long–long entanglement segment occurs through the CR-Rouse type mechanism that can never be faster than the intrinsic Rouse equilibration occurring at the time τ_e/υ_2^2, $\tau_{long-long\ eql}$ can be expressed as

$$\tau_{long-long\,eql} = \max(\tau_e Z_2'^2,\ \tau_{short-long} Z_2''^2) \tag{17a}$$

with

$$Z_2' = \min\left(\frac{1}{\upsilon_2}, Z_2\right), \quad Z_2'' = \min\left(\frac{\upsilon_1}{\upsilon_2}, Z_2\right) \tag{17b}$$

(Equation 17b has been introduced to include the extreme case of dilute long chain entangled only with the short chain ($1/\upsilon_2 > Z_2$ and $\upsilon_1/\upsilon_2 > Z_2$). For mutually entangled long chains having υ_2 well above $1/Z_2$, eq 17a gives $\tau_{long-long\ eql} = \tau_{short-long}\ (\upsilon_1/\upsilon_2)^2$, the Rouse-CR time for υ_1/υ_2 short–long entanglements.) . The CR-activated CLF of a specific molecular segment x is therefore expressed as

$$\tau_{CR\text{-}CLF}(x) = \tau_{long-long\,eql}\frac{9\pi^3}{16}(\upsilon_2 Z/2)^4 x^4 \tag{18}$$

which is then considered in eqs 13 and 14. Similarly, the reptation time of the long chains, which takes place after the CR-activated CLF and is the terminal relaxation process of the long chains, needs to account for the fact that the short chains are too long to behave as a real solvent and that a long–long entanglement segment needs a time $\tau_{long-long\ ent}$ to be equilibrated due to the release/formation of the short–long entanglements.[20,21] Therefore, eq 15 is rescaled as

$$\tau_{rept}(M, t) = \min((3\tau_e Z_2^3), (3(\tau_{long-long\,eql})(\upsilon_2 Z_2)^3)) \tag{19}$$

Equation 19 indicates that the chain reptates along the fully dilated tube if $3\tau_e Z_2^3 > \tau_{long-long\ eql}(\upsilon_2 Z_2)^3$, but reptation for this case is retarded due to the tension equilibration (with the charcateristic time $\tau_{long-long\ eql}$) and not governed by the intrinsic curvilinear diffusion coefficient D_c°. (This type of reptation is equivalent, in time scale, to the reptation along a partially dilated tube being associated with D_c°, as considered in previous studies.[21,39])

As illustrated in Figure 10, by using eqs 17–19, we are considering the chain motions at two different length scales,

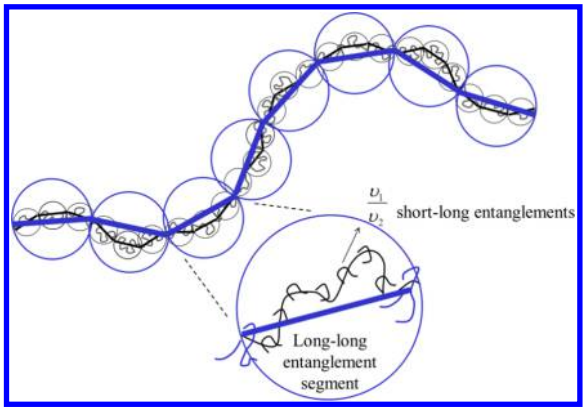

Figure 10. Illustration of the two length scales used for describing the motion of the long chains. Either the long chains mainly relax in the undilated tube, i.e., following eq 8b with $\Phi^* = 1$ and eq 9b (each entanglement segment is represented by a thin black line), or they mainly relax in the dilated tube, at the rhythm of the release/formation of the short–long entanglement segments, i.e., following eqs 17–19 (each long–long entanglement segment is represented by a thick blue line).

defined by M_e and M_e/υ_2. These two molecular segments are associated with a different equilibration time, equal to τ_e and $\tau_{long-long\ eql}$, respectively. While the first case is characterized by a short equilibration time of the segment unit, τ_e, but by a large number of segments, in the second case the equilibration time $\tau_{long-long\ eql}$ is much longer but the chains contain only few of these long–long segments. Therefore, depending on the blend composition and component molecular weights, the balance between the motions associated with these two length-scales is changed, and one or the other can become dominant.

It must be noted that while it contradicts the proposition of Doi et al.[40] to describe the CR mechanism in binary blends considering the chain motion at these two different length scales, this description is in line with the proposition of Viovy et al.,[41] who define two different types of chain motion, either along the undiluted (or skinny) tube or along the dilated tube. Also, they consider that the long chain motion along the dilated tube takes place at the rhythm of the short chain motion and is

dx.doi.org/10.1021/ma501566w | Macromolecules 2014, 47, 7653–7665

therefore much slower than the motion of the same long chain moving in a real solvent, as it is also proposed here. We can then conclude that this work is in agreement with the constraint release picture proposed by Viovy et al., even if differences appear in the way to define the equilibration time $\tau_{\text{long–long eql}}$ (which, for example, in the present work, depends on υ_1) and by the fact that we account for contour length fluctuations. On the other hand, eqs 18 and 19 are also in line with the work of Read et al.,[18] in which enhanced CLF is considered by renormalizing the diffusion constant at the chain ends.

In this study, the average lifetime of the short–long entanglement, $\tau_{\text{short–long}}$ appearing in eq 17a, was assumed to be independent of the long chain concentration, and its value is determined so as to best fit the data, as shown later in Figure 12. The $\tau_{\text{short–long}}$ value (= 1.5×10^{-5} s) obtained from this best-fitting method was satisfactorily close to that deduced from the data for the dielectric CR relaxation time $\tau_{\text{CR}}^{[\varepsilon]}$ of the *dilute* long PI chain entangled only with the short matrix PI chains:[16] $\tau_{\text{CR}}^{[\varepsilon]} = 0.16$ s for dilute PI308k in PI21k, based on the data of the second-moment average relaxation time given in ref 16, which gives $\tau_{\text{short–long}} \cong \tau_{\text{CR}}^{[\varepsilon]}/{Z_2}^2 \cong 2.4 \times 10^{-5}$ s being close to the value obtained from the fitting. (The best-fit value of $\tau_{\text{short–long}}$ depends on the choice of the functional form of $p_{\text{fluc}}^{[k]}(x_i, t)$ (eq 9a) and $p_{\text{CR-CLF}}^{[2]}(x_i,t)$ (eq 14). If some mode distribution is introduced for $p_{\text{fluc}}^{[k]}(x_i, t)$ and $p_{\text{CR-CLF}}^{[2]}(x_i,t)$, instead of the *approximate* single-exponential form[51] adopted in eqs 9a and 14, the best-fit value of $\tau_{\text{short–long}}$ could become even closer to the value deduced from the $\tau_{\text{CR}}^{[\varepsilon]}$ data.)

Strictly speaking, $\tau_{\text{short–long}}$ should increase with increasing concentration of the long chain because of the retardation of the short chain motion (due to suppression of CR/DTD for the short chain[39]). However, this increase is just moderate (within a factor of 2),[21] and incorporation of such moderate increase hardly affected the calculation results shown later in Figure 12. Thus, for simplicity and clarity of calculation, we assumed the constant $\tau_{\text{short–long}}$ value. The feature of $\tau_{\text{short–long}}$ is further discussed later in section IV.3.4.

While based on eqs 17–19, a good agreement between the experimental and calculated dielectric loss for the PI21/PI308 blends containing at least 5 wt % of long chains (see below, Figure 12), these equations do not take into account the fact that below a certain amount of long chains (defined as $\upsilon_2 Z_2 < 2$), the dilated tube does not exist anymore, and therefore, the CR-activated CLF process is not valid anymore, becoming virtually faster that the intrinsic Rouse relaxation of the chains. In order to account for this limitation, we impose that the long chains cannot relax through the CR-activated CLF process before the long–long entanglement segment is internally equilibrated, i.e., before the chain is able to relax in a dilated tube. To this end, in this study, we follow ref 52 and describe the CR-activated CLF in a new coordinate axis illustrated in Figure 11, which ensures that the CR-activated CLF starts only after $\tau_{\text{long–long eql}}$. Within this new axis, the coordinate y is determined by accounting for an extra (virtual) molecular segment of mass M^+, which is cast in a relationship

$$\tau_{\text{CR-CLF}}(y = x_{\text{end}}) = \tau_{\text{CR-CLF}}(x = 0) = \tau_{\text{long–long eql}} \qquad (20)$$

The coordinate of the extra segment in the new axis, $y = x_{\text{end}}$, is determined so as to allow the CR-activated CLF to start at $\tau_{\text{long–long eql}}$. Thus, for the long chain entangled with the short matrix chains, the characteristic time of the CR-activated CLF process appearing in eq 18, $\tau_{\text{CR-CLF}}$, is determined with the aid of the proportionality $p_{\text{CR-CLF}}(x) \propto y^4$ characteristic of the Rouse-CR process in the early stage.

The use of the new coordinate axis has negligible influences on $\tau_{\text{CR-CLF}}$ for a large volume fraction of the long chains, whereas the influence becomes significant for small υ_2 (<0.05). Indeed, for such small υ_2, the tube significantly dilates and the chains need a longer time before being able to fluctuate in this dilated tube (see eq 17), which can have repercussion on the CR-activated CLF on the *deeper* segments at $x \sim 1$. Indeed, for small υ_2, the necessary time for internal equilibration of a long–long entanglement segment becomes important, which delays the CR-activated CLF process. This delay of the CR-activated CLF will also depend on the time $\tau_{\text{short–long}}$, which is increased in the case of longer "short chains matrix".

For the PI308k/PI21k blends, the dielectric loss calculated with the aid of eqs 17, 18, and 19 are shown in Figure 12. The calculation agrees with the data very well in the entire range of υ_2 because it took into account the CR-CLF process and the essential fact that this process does not start before the internal equilibration of the long–long entanglement segment.

The dielectric data of the PI/PI blends are thus well described by our model considering the CR-activated CLF and reptation along the dilated tube that occurs with a certain delay (compared to CLF in a real solvent) due to the non-negligible time of the release/formation of the short–long entanglements.[20,21,38]

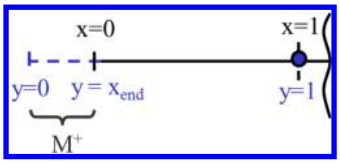

Figure 11. Cartoon representing the coordinate system y, which has been used to describe the CR-activated CLF. The mass M^+ is introduced in order to allow this CLF to start at a time $\tau_{\text{long–long ent}}$.

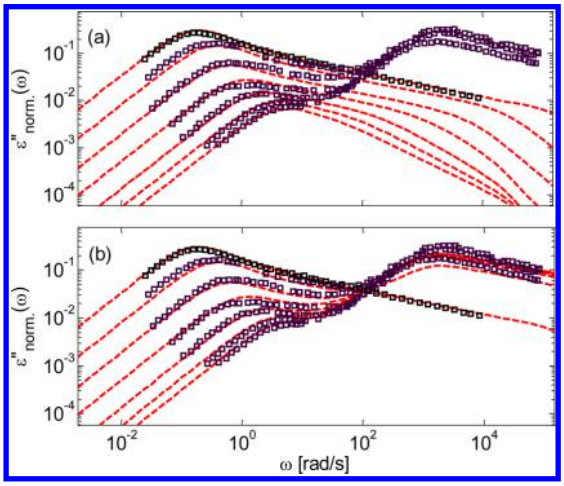

Figure 12. Comparison between normalized data of experimental and calculated dielectric loss for PI21 and PI308 (see Table 1) mixed in different proportions: 100%, 50%, 20%, 10%, 5%, 3%, and 2% of PI308. The calculation was made by considering the intrinsic Rouse CLF (see eq 12), CR-activated CLF in the coordinate axis y (see eqs 18 and 20), and reptation as described in eq 19, with $\tau_{\text{short–long}} = 1.5 \times 10^{-5}$ s. The calculated results are shown only for the contribution of the long component (a) or the contribution of both components (b).

dx.doi.org/10.1021/ma501566w | Macromolecules 2014, 47, 7653–7665

As a next step, it is interesting to see if the same model can also describe the viscoelastic data of the PI/PI blends. To do so, eq 6 (not eq 16) must be used together with eqs 4 and 5. The calculated results are shown in Figure 13: the calculation is

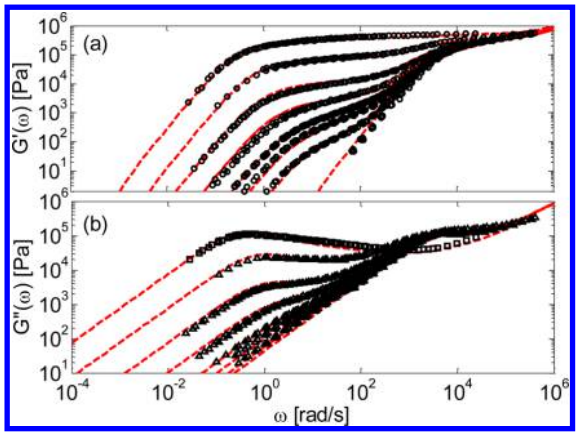

Figure 13. Comparison between experimental and calculated storage (a) and loss (b) moduli for PI21 and PI308 (see Table 1) mixed in different proportions: 100%, 50%, 20%, 10%, 5%, 3%, and 2% of PI308. The calculation was made by considering the intrinsic Rouse CLF (see eq 12), CR-activated CLF in the coordinate axis y (see eqs 18 and 20), and reptation as described in eq 19, with $\tau_{short-long} = 1.5 \times 10^{-5}$ s.

again in very good agreement with the data. In particular, the smooth transition observed between the reptation of the short chains and of the long chains, which corresponds to the transition between an effective dilution exponent α of 1 to an effective exponent of 4/3, is now well described. The good agreement for both dielectric and viscoelastic data also validates the (partial) DTD picture (see eq 6).

We now apply this model to predict the viscoelastic data of binary blends composed of PI329 and PI14, the latter having $M_1 \cong 3.6M_{e0}$, i.e., at the limit of being entangled.[49] Results are shown in Figure 14. Again, incorporation of the CR-activated CLF (eq 13) having the characteristic time given by eqs 17 gives a good agreement between the data in the dominant part of relaxation and the calculated curve.

IV.3.3. Test of Model for PBD/PBD Blends. Here, the model formulated/explained in the previous section is tested for the

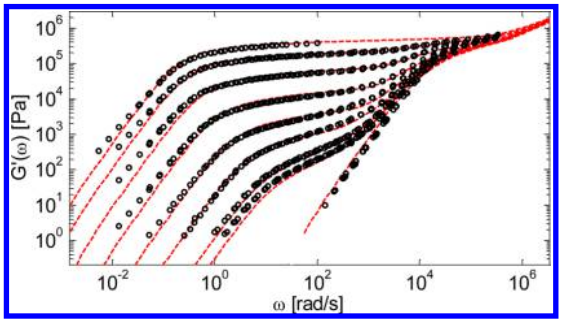

Figure 14. Comparison between calculated (curves) and measured (symbols) storage moduli for blends of PI14 and PI329 having various compositions, υ_2 (%) = 100 (bulk PI329), 70, 40, 20, 10, 5, 2, 1, and 0 (bulk PI14). The calculation was made by considering the intrinsic Rouse CLF (see eq 12), CR-activated CLF in the coordinate axis y (see eqs 18 and 20), and reptation as described in eq 19, with $\tau_{short-long} = 0.9 \times 10^{-5}$ s.

literature data for PBD/PBD blends containing the long components entangled with much shorter matrix component. Three different series of PBD blends, corresponding to three different values of the Graessley number (eq 3), are investigated, based on the same material parameters (see Table 2).

In Figure 15, the calculated viscoelastic curves and the data are shown for PBD550/PBD20 blends. By accounting for the

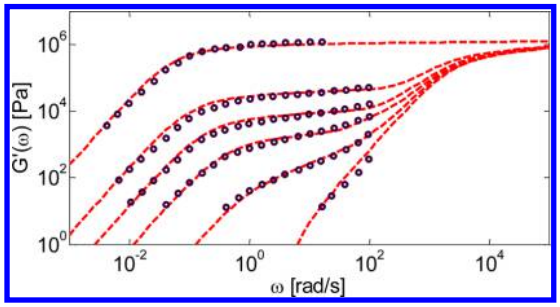

Figure 15. Comparison between experimental and calculated storage moduli for PBD20 and PBD550 (see Table 1) mixed in different proportions: 100%, 20%, 10%, 5%, 1%, and 0% of PBD550. The calculation was made by considering the intrinsic Rouse CLF (see eq 12), CR-activated CLF in the coordinate axis y (see eqs 18 and 20), and reptation as described in eq 19, with $\tau_{short-long} = 1.4 \times 10^{-6}$ s.

tension re-equilibration process through the CR-activated CLF (eqs 17−19), the model again describes the data very well. In particular, the level of the low-frequency plateau of G' is now correctly described, which was not the case in ref 14 based on usual assumption of tube models.

We now focus on PBD160/PBD25 blends. As mentioned in ref 15, these blends have the Graessley number very close to the critical value of 0.064 (definition by Park and Larson) above which the long chains are considered to reptate in a dilated tube. Park and Larson found a rather good agreement between their calculation and data by considering reptation in a skinny tube. However, they also showed that the relaxation times of the long chains becomes overestimated when the long chain concentration decreases, arguing that in this case one should probably consider an intermediate stage of the tube dilution. The same data have also been examined by Lee et al., who concluded—contrary to Park and Larson—that the long chain reptates along a dilated tube rather than a skinny tube.[48] This difference between the two conclusions was most probably due to the fact that Lee et al. used a different set of material parameters and a dilution exponent α equal to 1.3.[43]

Figure 16 compares our model calculation and the data for PBD160/PBD25 blends. The agreement with the data is again very good even for the "problematic" blend having the lowest content of long chains, $\upsilon_2 = 0.2$. In fact, the CR-activated CLF incorporated in our model has a significant effect on the relaxation function only for this 20% blend, and the effect becomes weaker and finally almost vanishes with increasing υ_2.

In Figure 17, our model is applied to bidisperse blends of PBD36 and PBD168. Compared to the blends examined in Figures 15 and 16, M_1 and M_2 are much closer to each other and the Graessley number is very small ($Gr = 0.08$) in the PBD168/PBD36 blends. Because of this feature, the equilibrium time of a long−long entanglement segments is too long to give any significant effect of the CR-activated CLF on the relaxation of the long chain relaxation. For this reason, the results shown in Figure 17 are equivalent to the results

dx.doi.org/10.1021/ma501566w | Macromolecules 2014, 47, 7653−7665

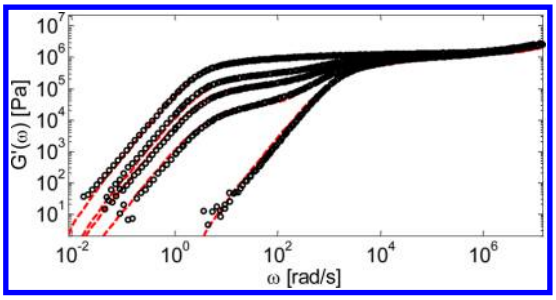

Figure 16. Comparison between experimental and calculated storage moduli for PBD25 and PBD160 (see Table 1) mixed in different proportions: 100%, 60%, 40%, 20%, and 0% of PBD160 (with T = 28 °C). The calculation was made by considering the intrinsic Rouse CLF (see eq 12), CR-activated CLF in the coordinate axis y (see eqs 18 and 20), and reptation as described in eq 19, with $\tau_{short-long} = 2 \times 10^{-6}$ s.

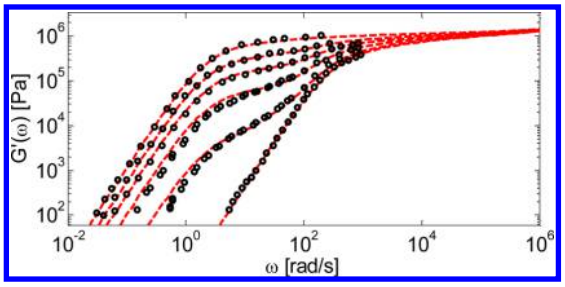

Figure 17. Comparison between experimental and calculated storage moduli for PBD36 and PBD168 (see Table 1) mixed in different proportions: 100%, 70%, 50%, 30%, 10%, and 0% of PBD160. The calculation was made by considering the intrinsic Rouse CLF (see eq 12), CR-activated CLF in the coordinate axis y (see eqs 18 and 20), and reptation as described in eq 19. However, for these blends, the influence of CR-activated CLF was negligible.

obtained without considering the CR-activated CLF (tension re-equilibration), contrary to all the other blends presented above. One can observe in Figure 17 that the calculation well describes the data, which lends support to the conclusion that the CR-activated CLF significantly influences the relaxation only for binary blends with well-separated molecular weights and a large *Gr*. It must be also noted that in ref 25 Wang et al. predicted the rheology of these same blends based on their hierarchical model and concluded that the model predictions of the storage modulus for moderate fractions of long chains were lower than the experimental data. This was most probably due to the fact that the dilution exponent of 1.3 was used, enhancing the CR effect from the short chains.

IV.3.4. Average Lifetime of a Short–Long Entanglement. As mentioned above, the average lifetime of a short–long entanglement, $\tau_{short-long}$, has been fixed by best fitting of the data with eq 17, assuming that it is a constant for each set of blends. Apart from the mixtures based on PBD36 and PBD168, for which the CR-activated CLF is not active, it appeared that for the blends analyzed here, this lifetime is relatively short, corresponding to several times of τ_e for equilibration of the entanglement segment. For the PI/PI blends, the $\tau_{short-long}$ values utilized in the best fitting were numerically close to the CR time data available for those blends. (Even closer agreement could be expected if we improve the *approximate* single-exponential form[51] adopted in eqs 9a and 14 and re-evaluate $\tau_{short-long}$ accordingly.) Nevertheless, it is desired to further analyze the dynamics of short–long entanglement relaxation to derive $\tau_{short-long}$ theoretically, rather than utilizing it as a fitting parameter. Further study is being planned along this line.

V. CONCLUSION

In this paper, we have investigated and modeled the viscoelastic properties of binary blends being composed of linear chains with well-separated molecular weights and having various compositions. These systems are indeed very suitable to test the validity and the limit of the constraint release and dynamic tube dilution processes, to study how the solvent effect from the short chains affects the relaxation of long chains, and to discuss the value of the dynamic dilution exponent α.

We first focused on binary blends composed of barely entangled short chains. In such a case, we have shown that a very good agreement between the tube model predictions and the experimental data is obtained if we account for the influence of the tension equilibration process along the long chains, which is modeled as the CR-activated CLF. In addition, in such a case, reptation is considered to take place along a fully dilated tube, as if the long chains were diluted in a real solvent. This allows us to show that this CR-activated CLF process speeds up the relaxation of the long chains, which naturally leads to an *effective* dilution exponent α equal to 4/3, despite the fact that the modeling is based on α = 1. This result is thus in agreement with the idea recently proposed in refs 20 and 21.

Then, we analyzed the rheological behavior of binary linear blends composed of entangled short chains. In such a case, we have shown that the CR-activated CLF also takes place during the relaxation of the long chains. However, it is necessary to include a delay time in this relaxation process, which represents the necessary time for the long chain to be able to fluctuate along their dilated tube and which is thus equal to the internal equilibration time of a long–long entanglement segment. In order to ensure the CR-activated CLF do not start before this delay time, we have used a new coordinate system, following ref 52. On the other hand, reptation is also considered in a fully dilated tube, but being retarded according to the rhythm of the release/formation of the short–long entanglements. This type of retarded reptation along the fully dilated tube is equivalent to the reptation with the intrinsic curvilinear diffusivity (no retardation in this sense) but occurring along a partially dilated tube, as considered in a recent study.[39]

This approach has been tested on several linear binary blends, showing an improved quality of the predictions compared to results previously obtained with tube models on the same blends. This allows us to conclude that with extreme binary blends as proposed in this work, the fast motions of the short chains are speeding up the relaxation of the long chains through the tension re-equilibration process, which can be described as CR-activated CLF. This process suffices to explain why a larger fraction of the long chains relaxes before their reptation, leading to an *effective* dilution exponent larger than 1 noted for the level of the low-frequency plateau modulus. Thus, this picture allows us to unify the different conclusions found about the exact value of this exponent. As a perspective, we would like to extend this work to the relaxation of star polymers, blended or not, with a shorter component.

AUTHOR INFORMATION

Corresponding Author

*E-mail evelyne.vanruymbeke@uclouvain.be (E.v.R.).

Notes

The authors declare no competing financial interest.

■ ACKNOWLEDGMENTS

The authors are very grateful to Dimitris Vlassopoulos and Johan Slot for helpful discussions. This work was partly supported by the Fonds National de la Recherche Scientifique (FNRS), the Dutch Polymer Institute (DPI), the Grant-in-Aid for Scientific Research (A) from MEXT, Japan (Grant No. 24245045), Grant-in-Aid for Scientific Research (C) from JSPS, Japan (Grant No. 24550135), and Collaborative Research Program of ICR, Kyoto University (Grant No. 2014-42).

■ REFERENCES

(1) Dealy, J. M.; Larson, R. G. *Structure and Rheology of Molten Polymers*; Hanser Verlag: Munich, 2006.
(2) Watanabe, H. *Prog. Polym. Sci.* **1999**, *24*, 1253.
(3) McLeish, T. C. B. *Adv. Phys.* **2002**, *51*, 1379.
(4) van Ruymbeke, E.; Slot, J. J. M.; Kapnistos, M.; Steeman, P. A. M. *Soft Matter* **2013**, *9* (29), 6921.
(5) Doi, M. *J. Polym. Sci., Polym. Phys. Ed.* **1983**, *21*, 667.
(6) de Gennes, P. G. *J. Chem. Phys.* **1971**, *55*, 527.
(7) Doi, M.; Edwards, S. F. *The Theory of Polymer Dynamics*; Oxford University Press: New York, 1986.
(8) des Cloizeaux, J. *Europhys. Lett.* **1988**, *5*, 437.
(9) Tsenoglou, C. *ACS Polym. Prepr.* **1987**, *28*, 185. Tsenoglou, C. *Macromolecules* **1991**, *24*, 1762.
(10) Marrucci, G. *J. Polym. Sci., Polym. Phys. Ed.* **1985**, *23*, 159.
(11) Milner, S. T.; McLeish, T. C. B. *Macromolecules* **1997**, *30*, 2159.
(12) Ball, R. C.; McLeish, T. C. B. *Macromolecules* **1989**, *22*, 1911.
(13) Struglinski, M. J.; Graessley, W. W. *Macromolecules* **1985**, *18*, 2630.
(14) Park, S. J.; Larson, R. G. *Macromolecules* **2004**, *37*, 597.
(15) Park, S. J.; Larson, R. G. *J. Rheol.* **2006**, *50*, 21.
(16) Watanabe, H.; Ishida, S.; Matsumiya, Y.; Inoue, T. *Macromolecules* **2004**, *37*, 1937.
(17) Watanabe, H.; Ishida, S.; Matsumiya, Y.; Inoue, T. *Macromolecules* **2004**, *37*, 6619.
(18) Read, D. J.; Jagannathan, K.; Sukumaran, S. K.; Auhl, D. *J. Rheol.* **2012**, *56*, 823.
(19) Khaliullin, R. N.; Schieber, J. D. *Macromolecules* **2010**, *43*, 6202.
(20) van Ruymbeke, E.; Masubuchi, Y.; Watanabe, H. *Macromolecules* **2012**, *45*, 2085.
(21) Watanabe, H.; Matsumiya, Y.; Van Ruymbeke, E. *Macromolecules* **2013**, *46*, 9296.
(22) Shivokhin, M. E.; van Ruymbeke, E.; Bailly, C.; Kouloumasis, D.; Hadjichristidis, N.; Likhtman, A. E. *Macromolecules* **2014**, *47*, 2451.
(23) Auhl, D.; Chambon, P.; McLeish, T. C. B.; Read, D. *Phys. Rev. Lett.* **2009**, *103*, 136001.
(24) Milner, S. T. *Macromolecules* **2005**, *38*, 4929.
(25) Wang, Z.; Chen, X.; Larson, R. G. *J. Rheol.* **2010**, *54*, 223. Larson, R. G. *Macromolecules* **2001**, *34*, 4556.
(26) Das, C.; Inkson, N. J.; Read, D. J.; Kelmanson, M. A.; McLeish, T. C. B. *J. Rheol.* **2006**, *50*, 207.
(27) van Ruymbeke, E.; Bailly, C.; Keunings, R.; Vlassopoulos, D. *Macromolecules* **2006**, *39*, 6248.
(28) Milner, S. T.; McLeish, T. C. B.; Young, R. N.; Johnson, J.; Hakiki, A. *Macromolecules* **1998**, *31*, 9345.
(29) Watanabe, H.; Matsumiva, Y.; van Ruymbeke, E.; Vlassopoulos, D.; Hadjichristidis, N. *Macromolecules* **2008**, *41*, 6110.
(30) Kapnistos, M.; Vlassopoulos, D.; Roovers, J.; Leal, L. G. *Macromolecules* **2005**, *38*, 7852. Kapnistos, M.; Koutalas, G.; Hadjichristidis, N.; Roovers, J.; Lohse, D. J.; Vlassopoulos, D. *Rheol. Acta* **2006**, *46*, 273.
(31) Ahmadi, M.; Bailly, C.; Keunings, R.; Nekoomanesh, M.; Arabi, H.; van Ruymbeke, E. *Macromolecules* **2011**, *44*, 647.
(32) Snijkers, F.; van Ruymbeke, E.; Kim, P.; Lee, H.; Nikopoulou, A.; Chang, T.; Hadjichristidis, N.; Pathak, J.; Vlassopoulos, D. *Macromolecules* **2011**, *44*, 8631.
(33) van Ruymbeke, E.; Orfanou, K.; Kapnistos, M.; Iatrou, H.; Pitsikalis, M.; Hadjichristidis, N.; Lohse, D. J.; Vlassopoulos, D. *Macromolecules* **2007**, *40*, 5941. van Ruymbeke, E.; Muliawan, E. B.; Hatzikiriakos, S. G.; Watanabe, H.; Hirao, A.; Vlassopoulos, D. *J. Rheol.* **2010**, *54*, 643.
(34) Rubinstein, M.; Colby, R. H. *Polymer Physics*; Oxford University Press: New York, 2003.
(35) Colby, R. H.; Rubinstein, M. *Macromolecules* **1990**, *23*, 2753.
(36) Raju, V. R.; Menezes, E. V.; Marin, G.; Graessley, W. W. *Macromolecules* **1981**, *14*, 1668.
(37) Masubuchi, Y.; Takimoto, J.-I.; Koyama, K.; Ianniruberto, G.; Marrucci, G.; Greco, F. *J. Chem. Phys.* **2001**, *115*, 4387. Masubuchi, Y.; Watanabe, H.; Ianniruberto, G.; Greco, F.; Marrucci, G. *Macromolecules* **2008**, *41*, 8275.
(38) Watanabe, H.; Urakawa, O.; Kotaka, T. *Macromolecules* **1994**, *27*, 3525.
(39) Matsumiya, Y.; Kumazawa, K.; Nagao, M.; Urakawa, O.; Watanabe, H. *Macromolecules* **2013**, *46*, 6067.
(40) Doi, M.; Graessley, W. W.; Helfand, E.; Pearson, D. S. *Macromolecules* **1987**, *20*, 1900.
(41) Viovy, J. L.; Rubinstein, M.; Colby, R. H. *Macromolecules* **1991**, *24*, 3587.
(42) Wang, S.; Wang, S. Q.; Halasa, A.; Hsu, W. L. *Macromolecules* **2003**, *36*, 5355.
(43) van Ruymbeke, E.; Liu, C. Y.; Bailly, C. Quantitative Tube Model Predictions for the Linear Viscoelasticity of Linear Polymers. In *Rheology Reviews*; Binding, D. M., Hudson, N. E., Keunings, R., Eds.; The British Society of Rheology: Buckinghamshire, 2007; pp 53−134.
(44) Watanabe, H.; Matsumiya, Y.; Osaki, K. *Macromolecules* **2000**, *33*, 499.
(45) Watanabe, H.; Matsumiya, Y.; Inoue, T. *Macromolecules* **2002**, *35*, 2339.
(46) Watanabe, H.; Sawada, T.; Matsumiya, Y. *Macromolecules* **2006**, *39*, 2553.
(47) van Ruymbeke, E.; Keunings, R.; Bailly, C. *J. Non-Newtonian Fluid Mech.* **2005**, *128*, 7.
(48) Lee, J. H.; Archer, L. A. *J. Polym. Sci., Part B: Polym. Phys.* **2001**, *39*, 2501.
(49) Sawada, T.; Qiao, X.; Watanabe, H. *Nihon Reorojo Gakkaishi (J. Soc. Rheol. Jpn.)* **2007**, *35*, 11 (see also Supporting Information of ref 39).
(50) Shchetnikava, V.; Slot, J. J. M.; van Ruymbeke, E. *Macromolecules* **2014**, *47*, 3350−3361.
(51) Likhtman, A. E.; McLeish, T. C. B. *Macromolecules* **2002**, *35*, 6332.
(52) van Ruymbeke, E.; Kapnistos, M.; Vlassopoulos, D.; Liu, C. Y.; Bailly, C. *Macromolecules* **2010**, *43*, 525.
(53) Larson, R. G.; Sridhar, T.; Leal, L. G.; McKinley, G. H.; Likhtman, A. E.; McLeish, T. C. B. *J. Rheol.* **2003**, *47*, 809.
(54) Inkson, N. J.; Graham, R. S.; McLeish, T. C. B.; Groves, D. J.; Fernyhough, C. M. *Macromolecules* **2006**, *39*, 4217.